Proceedings of the 28th IEEE
EMBS Annual International Conference
New York City, USA, Aug 30-Sept 3, 2006

Towards a Biomechanical-Based Method for Assessing Myocardial Tissue Viability

Cristian A. Linte[1,3], Marcin Wierzbicki[2,3], Usaf Aladl[3], Terry M. Peters[1,2,3] and Abbas Samani[1,2,3]
[1] Biomedical Engineering, University of Western Ontario, London, ON, Canada
[2] Medical Biophysics, University of Western Ontario, London, ON, Canada
[3] Imaging Research Laboratories, Robarts Research Institute, London, ON, Canada

Abstract—**This work presents the first steps towards the development and implementation of a novel 3D biomechanical-based method for assessing the viability of myocardial tissue, with particular interest for its application in myocardial infarction (MI) diagnosis. This assessment technique quantifies the myocardial contraction forces developed within the ventricular myofibrils in response to the electrophysiological stimulus. In this manuscript we provide a 3D finite element (FE) formulation of a contraction force reconstruction algorithm based on an inverse problem solution of linear elasticity, along with its implementation using clinical data. This algorithm has been applied to patient-specific models obtained by extracting anatomical features from high-resolution, high-contrast magnetic resonance (MR) cardiac images. The input consists of motion information extracted by nonrigid registration of the mid-diastole reference image to the remaining images of the 4D data set, acquired using ECG-gating throughout the cardiac cycle. The result consists of a display-map of the contraction force distribution superimposed on the anatomical ventricle model, which allows the clinician to identify regions of low contractility in the myocardium.**

Keywords—**myocardial viability assessment, cardiac imaging, cardiovascular biomechanics, finite element modeling.**

I. INTRODUCTION

Coronary artery disease, along with its acute condition of MI, is the most common cause of death in the developed world. Some of the clinical challenges that arise in MI diagnosis include size estimation and localization of the necrosis, as well as assessment of tissue damage reversibility. Early and accurate assessment is crucial for identifying appropriate therapeutic procedures that reduce patient trauma and healthcare cost.

Current noninvasive methods employed in myocardial viability assessment rely on various techniques, such as nuclear medicine, MRI and strain imaging. Positron emission tomography (PET) is the most advanced scintigraphic imaging tool developed for *in-vivo* assessment of cardiac physiology and biochemistry[1]. Current technology allows the measurement of tracer activity with high spatial and temporal resolution[2], making PET the gold-standard viability assessment method, offering well-validated information about the presence and extent of viable myocardium. Contrast-enhanced MR imaging is another powerful tool capable of providing information regarding the extent of acute and chronic MI[3]. The hyper-enhancement effect is ascribed to the increased concentration of contrast agent in the necrosed areas, due to a delay in its washout rate[4]. By analyzing the myocardial deformation patterns based on systolic peak strain rate measurements[5], ultrasound[6,7], along with recently developed motion acquisition techniques (MR tagging and phase-contrast)[8,9], also provide efficient distinction between normally contracting myocardial segments and chronically infracted ones. While clinically valuable, the above methods provide no quantitative biomechanical information of the myocardial tissue, or how its mechanical properties affect its contractile capabilities.

However, in our approach, we have developed a 3D biomechanical-based technique capable of quantifying the myocardial damage caused by infarction. Contraction forces generated by myocardial tissues are indicative of their viability, and thus can be regarded as a direct, quantitative measure of the tissue functionality. Based on the cardiac tissue physiology, the left ventricle myocardium contains a high density of muscle fibers, capable of outputting relatively mild, local contractions, but globally amplified by engaging a large ensemble of myofibrils[10]. Hence, the myocardium has been modeled as a deformable solid, self-driven by an internally generated force distributed throughout its volume. The myocardial displacements are assumed to be solely the effect of contraction forces.

II. METHODOLOGY

The contraction force reconstruction technique presented in this manuscript consists of three main components, discussed in detail in the upcoming sections.

A. Generation of the Anatomical Ventricle Model

A static anatomical ventricle model was generated by segmenting the mid-diastolic (MD) image from a sequence of 20 ECG-gated MR images, each depicting the heart at different time-points in the cardiac cycle[11]. The MD

image was chosen as reference due to its low susceptibility to motion artifacts. Upon manual segmentation on a slice-by-slice basis, a static 3D surface model of the ventricle was created using surface triangulation. Employing a commercial meshing software, the surface model was converted to a 3D volumetric model, by performing a FE discretization of the 3D model, as shown in Fig. 1 below.

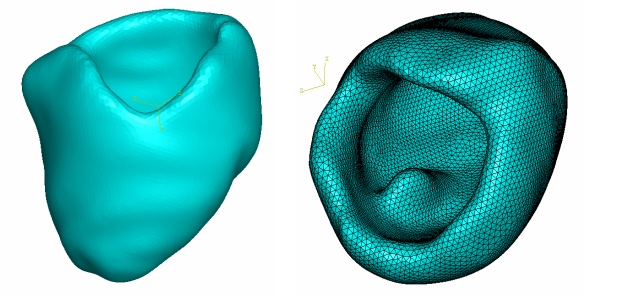

a) b)

Figure 1. Static patient-specific anatomical ventricle model generated by segmentation of the MD image from the 4D data set: a) rendered 3D ventricle model (left) ; b) rendered 3D ventricle model showing the FE mesh (right).

B. Cardiac Motion Extraction

The dynamic patient-specific model was obtained by animating the static model using cardiac motion information extracted using nonrigid registration. The registration algorithm follows a Free Form Deformation (FFD) approach, in which a 3D grid of points is overlaid on the 3D image to be registered. The nodal displacement vectors were estimated as the deformation required in the surrounding region to match this same particular region of the target image, therefore maximizing the Normalized Mutual Information (NMI) between the source and target image[11]. The frame-to frame motion vector $T_{0\text{-}N}$ was obtained by registering the MD image to each of the remaining 19 frames in the data set (Fig. 2). The ventricular motion was reconstructed by sequentially applying the registration transformations to the static model.

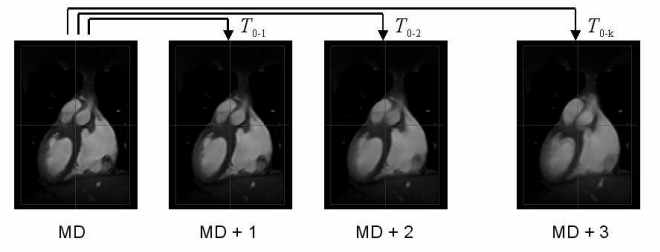

Figure 2. Registration scheme used to determine the motion vector ($T_{0\text{-}k}$) that maps the heart image from the mid-diastolic (MD) frame to the image form the k-th frame in the 4D data set, where k = 1 to 19.

C. 3D Inverse Algorithm

The inverse algorithm is the key component of the force reconstruction technique; it is driven by the continuum mechanics equation governing linear elastic isotropic behavior, also known as the Navier equation (1)

$$\frac{E}{2(1+\upsilon)}\nabla^2 U+\frac{E}{2(1+\upsilon)(1-2\upsilon)}\nabla(\nabla\cdot U)+f=\rho\cdot\partial_t^2 U \qquad (1)$$

where, E is the tissue elastic modulus (30 kPa)[10], ρ is the tissue density (1.05 g/cm^3), υ is its Poisson's ratio (0.495), $U = \{u\ v\ w\}^T$ is the displacement vector field, $f = \{f_x f_y f_z\}^T$ is the body force per unit volume. The algorithm uses the myocardial displacement field previously obtained as input, and it retrieves the contraction force components throughout the entire computational domain, by inverting the above equation.

In contrast to the 2D version of the force reconstruction algorithm described in our previous work (MI06-6143-97 SPIE2006), this 3D implementation is based on a finite element formulation, as opposed to the previous finite difference method of solution employed in the 2D formulation.

In order to obtain the finite element formulation, the Principle of Virtual Work (PVW) was applied to the spatial components form of the elasticity equation (due to space limitations, only the x-component is shown) as follows,

$$\iiint_V\left(\frac{\partial\sigma_x}{\partial x}+\frac{\partial\tau_{xy}}{\partial y}+\frac{\partial\tau_{xz}}{\partial z}+f_x-\rho\cdot\ddot{u}\right)\delta u\,dV=0 \qquad (2)$$

where $\{\sigma\}$represents the stress vector, $\ddot{u}$ is the x-component of nodal acceleration and δu represents a virtual displacement in the x-direction.

Using fundamental continuum mechanics principles the PVW equation can be expressed in terms of the surface traction T and virtual strain $\delta\varepsilon$. Upon assembling the x-, y- and z-components and noting that the surface traction vector can be omitted since it serves no purpose to our deformable model, the PWV can be further manipulated using the generalized Hooke's Law[12]. The periodic nature of the cardiac cycle allows us to express the nodal acceleration component in the form$\{\ddot{U}\}=-\omega^2\{U\}$.

The linear shape functions used in the approximation stage were carefully chosen to reduce the computational difficulty[12]:

$$\{U\}=\left\{\sum_{i=1}^{4}x_i N_i \quad \sum_{i=1}^{4}y_i N_i \quad \sum_{i=1}^{4}z_i N_i\right\}^T=[H]\cdot\{d\} \qquad (3)$$

The elements were mapped from their global coordinate system (x,y,z), to a master element in a local coordinate

system *(p,q,r)*. A Jacobian matrix was required to assist in the coordinate mapping, computed as follows:

$$\begin{bmatrix} \frac{\partial \circ}{\partial p} \\ \frac{\partial \circ}{\partial q} \\ \frac{\partial \circ}{\partial r} \end{bmatrix} = \begin{bmatrix} \frac{\partial x}{\partial p} & \frac{\partial y}{\partial p} & \frac{\partial z}{\partial p} \\ \frac{\partial x}{\partial q} & \frac{\partial y}{\partial q} & \frac{\partial z}{\partial q} \\ \frac{\partial x}{\partial r} & \frac{\partial y}{\partial r} & \frac{\partial z}{\partial r} \end{bmatrix} \cdot \begin{bmatrix} \frac{\partial \circ}{\partial x} \\ \frac{\partial \circ}{\partial y} \\ \frac{\partial \circ}{\partial z} \end{bmatrix}, \quad J = \begin{bmatrix} \frac{\partial x}{\partial p} & \frac{\partial y}{\partial p} & \frac{\partial z}{\partial p} \\ \frac{\partial x}{\partial q} & \frac{\partial y}{\partial q} & \frac{\partial z}{\partial q} \\ \frac{\partial x}{\partial r} & \frac{\partial y}{\partial r} & \frac{\partial z}{\partial r} \end{bmatrix} \tag{4}$$

Upon the incorporation of the shape functions, the PWV expression evolves to the following form[12],

$$\left[\iiint_V \{\delta d\}^T [B]^T [E][B] dV - \omega^2 \iiint_V \rho \{\delta d\}^T [H]^T [H] dV \right] \{d\} = \iiint_V \{\delta d\}^T [H]^T [H] \{f\} dV \tag{5}$$

One last simplification allowed us to rewrite the above equation in the final form,

$$\{F\} = \left[[K] - \omega^2 [M] \right] \{d\} \tag{6}$$

which retrieves the desired elemental contraction force vector. The overall force distribution is obtained by assembling the contraction force contribution from all elements in the model according to the connectivity map.

III. Results

The FE biomechanics-based inverse algorithm was employed in reconstructing the contraction force distribution in the myocardium at 19 stages in the cardiac cycle. The motion information was extracted from the nonrigid registration of the MD image to the remaining 19 ECG-gated MR images acquired as described in the previous section. Each of the frames displays the contraction force distribution throughout the deformed ventricle at a particular time point in the cardiac cycle, leading to the development of a dynamic model that superimposes the contraction force information onto the deformed volumetric geometry.

The contraction force magnitude is proportionally quantified using the element color intensity, encoded by a respective colorbar. Due to space limitations, contraction force reconstructions from 3 of the 19 cardiac frames are illustrated below. In order to clearly display myocardial contractile activity, the frames selected embrace both the diastolic and systolic cardiac phases.

By visual inspection of the presented diagrams, the intensity of the myocardial contraction forces can be easily noticed. Fig. 3 depicts the myocardium during the diastolic phase, when passive ventricular filling occurs due to the pressure gradient between the left atrium and the left ventricle. The myocardial muscle is relaxed and no mechanical work is performed.

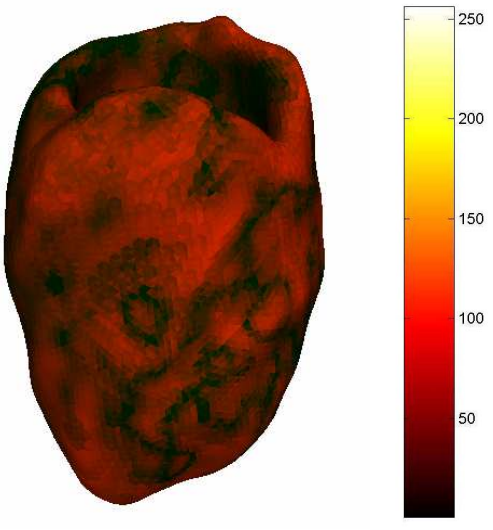

Figure 3. Map of the contraction force distribution magnitude within the myocardium at mid-diastole (MD).

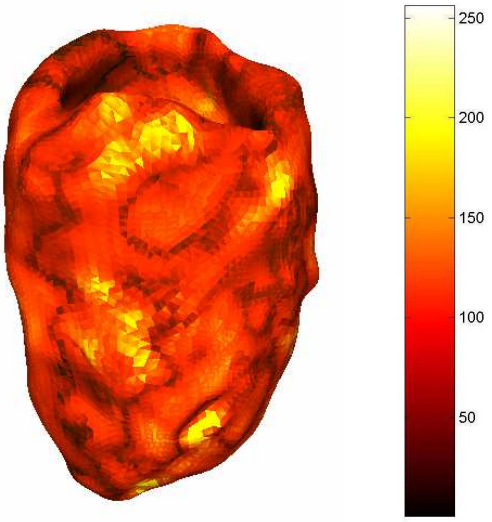

Figure 4. Map of the contraction force distribution magnitude within the myocardium at an intermediate stage between diastole and systole, referred to as contraction initiation (CI).

During the contraction initiation phase (Fig. 4), the muscle fibers in the ventricle wall start to shorten, increasing the magnitude of the internally generated force. At peak systole (Fig. 5) the myofibers experience the highest state of strain and the internal contraction force reaches its maximum providing a strong contraction throughout the ventricle. After the systolic phase, the tissue starts relaxing towards diastole, giving rise to another cardiac cycle.

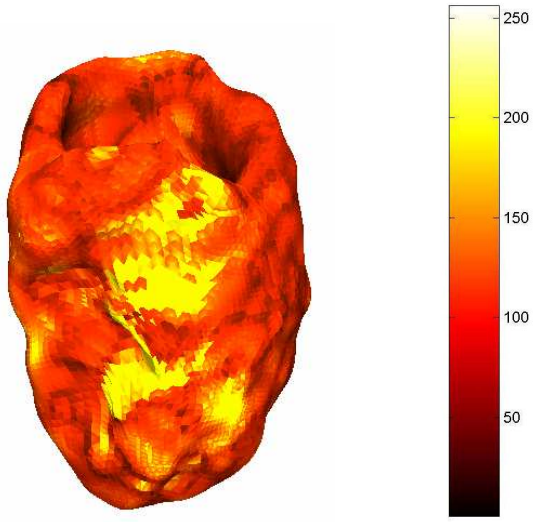

Figure 5. Map of the contraction force distribution magnitude within the myocardium at peak-systole (PS).

IV. Discussion

The contraction force reconstruction algorithm presented in this paper sets the ground for the development of a novel, quantitative, minimally invasive technique for assessing myocardial tissue viability. Furthermore, this method takes into account the biomechanical behavior of the cardiac muscle, and provides direct information with respect to the tissue functionality only based on a myocardial displacement field, which can be acquired using conventional medical imaging modalities.

In order to better display the contraction force field, an additional visualization step will overlay directional information of the vector field onto the ventricle. This will allow the user to better understand the complex cardiac motion, and clearly distinguish the motion patters at any stage in the cardiac cycle, by depicting the contraction or relaxation of particular myocardial regions.

Before adding more complex features to the biomechanical model used in this inverse problem formulation (e.g. tissue anisotropy), our next objective is to validate this technique. For this purpose, anatomical maps displaying the electrophysiological patterns are of great interest; in addition, a study including healthy and MI patients will further allow us to assess the plausibility of our algorithm.

V. Conclusion

In this work, a 3D inverse algorithm for reconstructing the myocardial contraction force distribution was developed. As a first approximation, our method currently assumes a linear isotropic tissue behavior, and the reconstructions are performed using fundamental linear elasticity principles. However, a more complex formulation is required to model the myocardial tissue, including aspects such as nonlinearity, finite deformation, and transverse isotropic tissue properties. Our results are encouraging and while qualitatively reasonable, more work is under way towards their quantitative assessment.

Acknowledgments

Cristian A. Linte thanks Dr. Mark Wachowiak, Dr. Hualiang Zhong, John Moore and Chris Wedlake for helpful discussions and advice, as well the Canadian Institute of Health Research (CIHR) and the Natural Sciences and Engineering Research Council (NSERC) for their financial support.

References

[1] Matsunari, I., Taki, J., Nakajima, K., Tonami, N., and Hisada, K., "Myocardial viability assessment using nuclear imaging," *Ann. Nucl. Med.*, vol. 17, no. 3, pp. 169-179, May 2003.

[2] Pirich, C. and Schwaiger, M., "The clinical role of positron emission tomography in management of the cardiac patient," *Rev. Port. Cardiol.*, vol. 19 Suppl 1, pp. I89-100, Feb. 2000.

[3] Hillenbrand, H. B., Kim, R. J., Parker, M. A., Fieno, D. S., and Judd, R. M., "Early assessment of myocardial salvage by contrast-enhanced magnetic resonance imaging," *Circulation*, vol. 102, no. 14, pp. 1678-1683, Oct. 2000.

[4] Mahnken, A. H., Koos, R., Katoh, M., Wildberger, J. E., Spuentrup, E., Buecker, A., Gunther, R. W., and Kuhl, H. P., "Assessment of myocardial viability in reperfused acute myocardial infarction using 16-slice computed tomography in comparison to magnetic resonance imaging," *J. Am. Coll. Cardiol.*, vol. 45, no. 12, pp. 2042-2047, June 2005.

[5] Voigt, J. U., Arnold, M. F., Karlsson, M., Hubbert, L., Kukulski, T., Hatle, L., and Sutherland, G. R., "Assessment of regional longitudinal myocardial strain rate derived from doppler myocardial imaging indexes in normal and infarcted myocardium," *J. Am. Soc. Echocardiogr.*, vol. 13, no. 6, pp. 588-598, June 2000.

[6] Urheim, S., Edvardsen, T., Torp, H., Angelsen, B., and Smiseth, O. A., "Myocardial strain by Doppler echocardiography. Validation of a new method to quantify regional myocardial function," *Circulation*, vol. 102, no. 10, pp. 1158-1164, Sept. 2000.

[7] Stoylen, A., Heimdal, A., Bjornstad, K., Torp, H. G., and Skjaerpe, T., "Strain Rate Imaging by Ultrasound in the Diagnosis of Regional Dysfunction of the Left Ventricle," *Echocardiography.*, vol. 16, no. 4, pp. 321-329, May 1999.

[8] Axel, L. and Dougherty, L., "MR imaging of motion with spatial modulation of magnetization," *Radiology*, vol. 171, no. 3, pp. 841-845, June 1989.

[9] McVeigh, E. R., "MRI of myocardial function: motion tracking techniques," *Magn Reson. Imaging*, vol. 14, no. 2, pp. 137-150, 1996.

[10] Humphrey J.D., *Cardiovascular Solid Mechanics: Cells, Tissues and Organs*, Springer - Verlag, Apr. 2002.

[11] Wierzbicki, M., Drangova, M., Guiraudon, G., and Peters, T., "Validation of dynamic heart models obtained using non-linear registration for virtual reality training, planning, and guidance of minimally invasive cardiac surgeries," *Med. Image Anal.*, vol. 8, no. 3, pp. 387-401, Sept. 2004.

[12] Bathe K.J., *Finite Element Procedures in Engineering Analysis*, Englewood Cliffs, NJ: Prentice Hall, Feb. 1996.